AD-A073 113   LOCKHEED MISSILES AND SPACE CO INC PALO ALTO CALIF PA--ETC   F/G 4/1
COORDINATED DATA ANALYSIS OF ONR-118 DATA.(U)
AUG 78   R G JOHNSON, R D SHARP, E G SHELLEY   N00014-77-C-0600
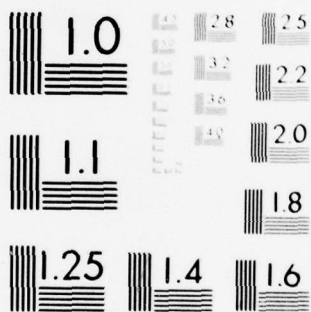UNCLASSIFIED   LMSC/D626959   NL

1 OF 1

AD
A073113

END
DATE
FILMED
9-79

DDC

1.0

28   25
3.2
36   22

1.1   20

1.8

1.25   1.4   1.6

MICROCOPY RESOLUTION TEST CHART
NATIONAL BUREAU OF STANDARDS 1963 A

LOCKHEED
MISSILES & SPACE COMPANY, INC. • SUNNYVALE, CALIFORNIA

DDC

AUG 21 1979

RECEIVED

FINAL REPORT

Coordinated Data Analyses
of ONR-118 Data

Prepared by

R. D. Sharp, R. G. Johnson and E. G. Shelley

Lockheed Palo Alto Research Laboratory
3251 Hanover Street
Palo Alto, California 94304

REPORT DOCUMENTATION PAGE		READ INSTRUCTIONS BEFORE COMPLETING FORM
1. REPORT NUMBER 087-183-8-78	2. GOVT ACCESSION NO.	3. RECIPIENT'S CATALOG NUMBER
4. TITLE (and Subtitle) Coordinated Data Analysis of ONR-118 Data		5. TYPE OF REPORT & PERIOD COVERED Final Report
		6. PERFORMING ORG. REPORT NUMBER LMSC/D626959
7. AUTHOR(s) R. G. Johnson, R. D. Sharp and E. G. Shelley		8. CONTRACT OR GRANT NUMBER(s) N00014-77-C-0600
9. PERFORMING ORGANIZATION NAME AND ADDRESS Lockheed Palo Alto Research Laboratory 3251 Hanover Street, Dept. 52-12, Bldg. 205 Palo Alto, California 94304		10. PROGRAM ELEMENT, PROJECT, TASK AREA & WORK UNIT NUMBERS NR 087-183
11. CONTROLLING OFFICE NAME AND ADDRESS Office of Naval Research Code 465 Arlington, Virginia 22217		12. REPORT DATE August 1978
		13. NUMBER OF PAGES 28
14. MONITORING AGENCY NAME & ADDRESS(if different from Controlling Office)		15. SECURITY CLASS. (of this report) Unclassified
		15a. DECLASSIFICATION/DOWNGRADING SCHEDULE

16. DISTRIBUTION STATEMENT (of this Report)

Approved for public release and sale; distribution unlimited.

17. DISTRIBUTION STATEMENT (of the abstract entered in Block 20, if different from Report)

18. SUPPLEMENTARY NOTES

19. KEY WORDS (Continue on reverse side if necessary and identify by block number)

ionospheric disturbance phenomena, S-33 satellite data, Chatanika radar

20. ABSTRACT (Continue on reverse side if necessary and identify by block number)

This is the final report of a program to study the physical causes of ionospheric scintillation and disturbance phenomena by performing coordinated observations of the energetic particle inputs to the disturbance region and the resulting disturbance phenomena as observed in the ionosphere.

DD FORM 1473 EDITION OF 1 NOV 65 IS OBSOLETE
1 JAN 73
S/N 0102-014-6601

TABLE OF CONTENTS

Accession For

NTIS GRA&I	☑
DDC TAB	☐
Unannounced	
Justification	

By

Distribution/

Availability Codes

| Dist | Avail and/or special |
| A | |

ii

Introduction

This was a program to study the physical causes of ionospheric scintillation and disturbance phenomena by performing coordinated observations of the energetic particle inputs to the disturbance region and the resulting disturbance phenomena as observed in the ionosphere.

An ONR funded instrument to measure energetic ions and electrons was launched aboard the S3-3 Air Force satellite in July 1976 into an elliptical polar orbit with apogee at 8050 km and perigee at 260 km. The instrument has provided excellent data since it was turned on four days after launch and is still operating successfully. It measures the composition of ions in the mass range from 1 to 150 a.m.u. over the energy range from 0.5 to 16 keV. Electrons are measured over the range from 0.1 to 20 keV. Magnetospheric electric field data obtained with an ONR sponsored experiment on the same satellite are being acquired by the University of California (Dr. F. S. Mozer). Under this program data from these S3-3 experiments coordinated with the WIDEBAND II experiment and the Chatanika incoherent scatter radar facility have been acquired, and data from the Lockheed experiment has been surveyed and analyzed. Coordinated data have also been acquired with the ion and electron spectrometers in the DARPA funded payload aboard the Air Force P72-1 satellite which is in a near circular polar orbit at 750 km. Electrons are measured over the energy range from 0.1 to 40 keV and ions over the range 15 to 1000 keV (without mass discrimination) on this satellite.

Technical Activities

During the period of this contract we maintained contact with scientific personnel at Stanford Research Institute (S.R.I.) and Physical Dynamics, Inc. (P.D.)(Drs. R. Vondrack, C. Rino, O. de la Beaujardierre and E. Fremouw) in order to determine the relevant operational periods of the Chatanika radar facility and the Wideband II satellite. We then provided technical planning

1

and liaison with the Air Force Satellite Control Facility in order to maximize the S3-3 and P72-1 satellite data coverage at the times and locations of coordination. From these and earlier coordinations we selected a list of 40 periods when data from one of the Lockheed experiments were acquired and provided these to our colleagues at SRI and PD. A subset of 25 events was selected on the basis of the availability of good Wideband and/or Chatanika data and the data from these cases were surveyed to assess the quality, quantity and usefulness of the data. In cooperation, primarily with Dr. Vondrack of SRI, we then selected 6 cases for detailed quantitative analysis. We computed energy spectra with 0.5 second time resolution and angular distributions with approximately 10 second time resolution for the invariant latitude range 62° to 68° over Chatanika for these cases and provided these data to Dr. Vondrack. The Berkeley experimenters have also provided the electric field data for these cases.

RESULTS

An example of the combined data sets from one event is shown in Figures 1 and 2. Figure 1 provided by Dr. de la Beaujardierre shows the Wideband scintillation data in the upper panel; the total electron content in the central panel, and the Chatanika electron/density data in the lower panel. The low latitude, high altitude enhancement in electron density in the Chatanika data is a common feature which is generally associated with a scintillation enhancement as observed by Wideband. (R. Vondrack, private communication). In this case it appears to be spatially associated with the signature of the inner edge of the plasma sheet in the S3-3 electron data shown in the bottom four panels of Figure 2. (A detailed description of the quantities plotted in Figure 2 is contained in Sharp, et al.)* Note the field aligned electrons seen in CMEB and CMEC at about 69° invariant latitude (ILA). These are a low altitude signature of the high altitude auroral accel-

*J. Geophys. Res. 84, 480, 1979.

eration events discovered by the S3-3 satellite and described in Sharp, et al (1979).

The principle result of the coordinated study was the determination of the detailed particle and field parameters associated with an auroral feature which may be a precursor of some auroral substorms. These results are described in Appendix A.

In addition to the analysis of the coordinated observations we have also performed a limited statistical study on a number of the high altitude acceleration events mentioned in connection with Figure 1 in order to try to advance our understanding of the physical mechanisms responsible for auroral ionospheric disturbance phenomena. Upflowing ion events (UFI) were selected from a year's data (July 1976 to July 1977) which give complete coverage of latitude and local time. In order to reduce possible variations related to altitude or magnetic local time only those events were considered which occurred between 1800 and 2400 magnetic local time and above 6000 km. Since most of the events occur in this region, the data base was still substantial. Some of the events were observed for too short a time to give confidence that the electron measurements were of the pitch angle distributions associated with the ions and not temporal or spacial variations. In order to avoid possible confusing data all events were rejected which did not last for at least four spins, about 75 seconds. Events were also rejected if they were badly contaminated by telemetry noise. After this, 44 events remained.

For each spin the upflowing ions, precipitating electrons with pitch angles between 0° and 20° and trapped electrons with pitch angles between 80° and 100° were separated out. Only protons and singly charged oxygen ions were considered in view of the comparative rarity of upflowing helium ions. For both electrons and ions the following parameters were computed; number flux, energy flux, number density; all three integrated over energy, and average energy. The contribution of the electrons to the upward current was also found.

3

All these parameters were then plotted against each other and correlation
coefficients and regression lines evaluated in an attempt to detect relation-
ships between them. All the initial plots showed very considerable scatter
and a number of selection procedures allowed the relationships to show more
clearly.

On many of the spins the number of counts recorded by the ion mass spectro-
meters was low, so in order to limit the uncertainties due to counting stat-
istics only those spins were accepted for which the number of counts exceeded
a minimum. Values of minimum were chosen to give a substantial reduction in
scatter while still not unreasonably reducing the number of data points.
For protons the minimum count used was 10 and for oxygen ions, 5.

Since in one spin, measurements of the ion flux were made at only three ener-
gies and the ion energy spectra were peaked, the estimates of integrated flux
and mean energy were poor, especially in cases where the width at half maximum
of the energy spectrum was less than 75% of its mean energy. In these cases,
the spectrum is too narrow for more than one ion mass spectrometer to detect
ions. This measurement is unlikely to be near the peak of the spectrum,
which makes it useless as a measure of flux, although it still gives a rough
indication of energy. A much better estimate could have been made by using
all the twelve energy settings of the ion mass spectrometers. However, this
would have taken four spins to complete, and the ion or electron characteristics
usually changed substantially during that time.

The Aerospace experiment on S3-3 was able to obtain detailed ion energy spectra
with better time resolution but without mass separation. Their measurements
of upflowing ion energy spectra indicate that the widths of the spectra are
usually about the same as their mean energies. Such a width would allow at
least two of the spectrometers to obtain data, and this was taken as a minimum
requirement which would select the better measurements without leaving a data
set which was untypical of the general population. With this restriction it
was estimated that the errors introduced by the measurement system would not

4

exceed 30% of the ion energy or 50% for the fluxes, and in most cases would be better than this.

The results of the study are as follows. Proton number fluxes ranged from the threshold of the instrument, about 2.10^6 cm^{-2} str^{-1} s^{-1}, to a maximum of 5.10^8 while the flux of oxygen ions only reached a tenth of this. In both cases the frequency of occurrence fell rapidly with increasing flux, indicating that upflowing ions most commonly have fluxes near or below 10^6. Although proton fluxes were on the average larger than fluxes of oxygen ions, in individual cases the fluxes appeared to be quite independent of each other. This would be consistent with independent source plasmas.

Ions were observed with energies throughout the range of the instrument. Figure 3 shows the distribution of frequency occurrence of energies. The response of the instrument combined with the selection criteria distorts the distribution to some extent but not sufficiently to change their general character, which show the oxygen ions to be more energetic than the protons. This is true in individual cases as well as statistically as can be seen in Figure 4 where proton energy is plotted against the energy of oxygen ions, each point representing an individual spin. This indicates that the oxygen energy almost always exceeds that of the protons and is usually twice as great. Although the correlation is statistically significant (at 1%) there is still considerable scatter. A computer simulation of the energy estimation system suggested that over half of the scatter can be attributed to the inaccuracies in the estimation of energy. Had all the scatter been attributable to this cause it would be reasonable to conclude that both species of ions gained their energy from the same, or closely related, mechanisms. However, the data seem to allow the possibility of a separate mechanism which acts predominantly on one species.

Both trapped and precipitating electrons were examined when upflowing protons and oxygen ions were present. Their energies and fluxes are displayed in Figures 5 and 6. In most cases the electrons are isotropic within a factor of two, although some cases are markedly anisotropic. The flux maximizes

5

along the field lines in some instances and perpendicular to them in others. The correspondence between the energies of precipitating and trapped electrons is even more marked than the isotropy which strongly suggests that they are from the same population. This conclusion is supported by the relationships between the ions and electrons which were the same for both precipitating and trapped electrons.

The degree of isotropy is similar to the results obtained by Paschmann, et al* for the general auroral electron population. However, the range of flux in upflowing ion events is much more limited than is usual for auroral electrons. They reached a maximum of about 10^9 cm^{-2} str^{-1} s^{-1} and did not fall below 3.10^7 although the dynamic range of the instrument was 10^5 to 10^{11} and in the absence of upflowing ions the electron fluxes ranged down to 10^6 and Paschmann recorded fluxes between 10^9 and 5.10^6, the threshold of his instrument, for more general auroral conditions.

The present study has not revealed any way in which the integrated electron flux is related to the ions except for the limit on its range. However, the average electron energy is well correlated with the average ion energy. Figure 7 shows a loose linear relationship between the energies of oxygen ions and of trapped electrons. On the average, the ions and electrons have the same energy, although, in individual spins, there is as much as a factor of two between them. Since the electron measurements are relatively good most of the scatter represents real variability. Similar relationships were found for both species of ion and both trapped and precipitating electrons.

If the ions and electrons are both accelerated by an electrostatic field, which extends above and below the satellite, then the linear relationship between ion and electron energies is not what would be expected if the field region was of limited extent. In such circumstances the proportions of the potential above and below the satellite, and so the ratio of the electron and ion energies,

*J. Geophys. Res. 77, 6111, 1972.

6

will depend on the altitude of the satellite and will tend to produce an inverse relationship between the electron and ion energies. This is not what is observed, and moreover, there is no evidence of any variation of the relationship with satellite altitude over the range of 6000 km to 8000 km which leads to the tentative conclusion that the extent of the field region must be large compared with the 2000 km variation of the altitude of these observations. Further work will be required to substantiate this conclusion and to determine other properties of the auroral acceleration mechanism.

CONCLUSIONS

The observations from the S3-3 satellite have produced a major breakthrough in our knowledge of fundamental plasma processes by discovering a number of important hot plasma phenomena whose existence had previously been unknown. These phenomena have no known counterparts at low latitudes. They are directly relevant to DNA's interests in ionospheric instabilities which can cause irregularities leading to the disruptions of radar and communications systems. The newly discovered ionospheric acceleration mechanisms are also directly relevant to the transport, energy transfer, and dispersal of debris in a weapons environment.
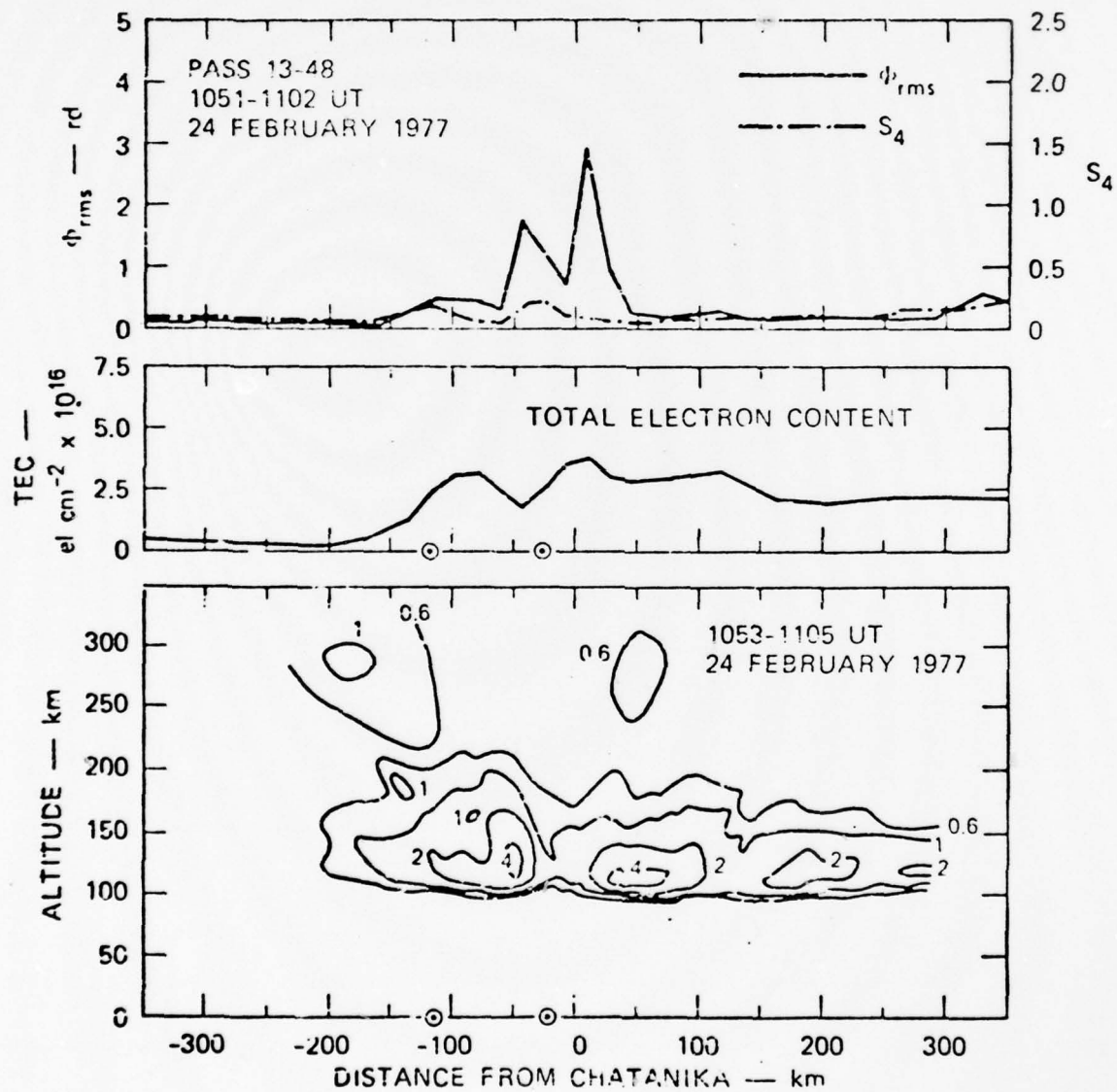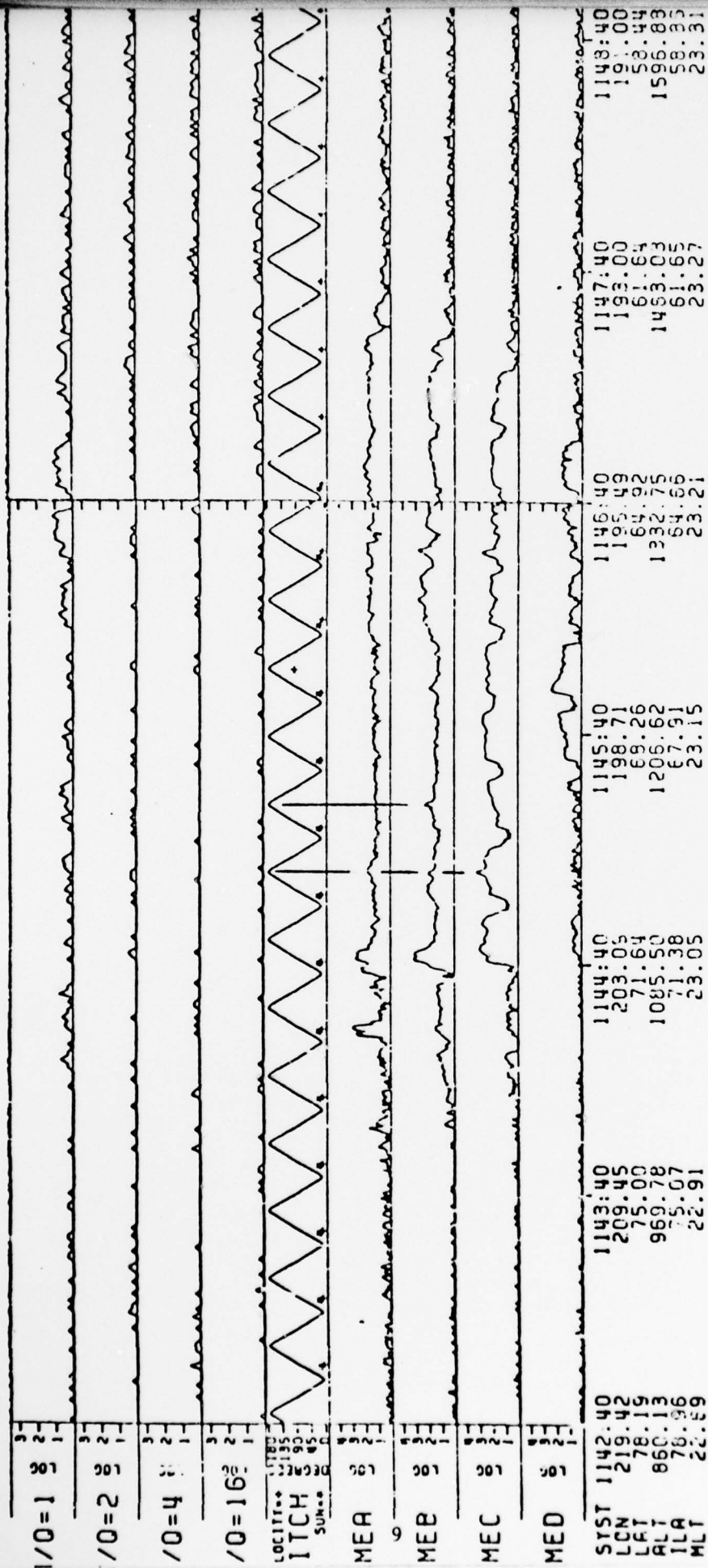
7

PASS 13-48
1051-1102 UT
24 FEBRUARY 1977

ϕ_{rms}

S_4

5

4

3

2

1

0

ϕ_{rms} — rd

2.5

2.0

1.5

1.0

0.5

0

S_4

TOTAL ELECTRON CONTENT

7.5

5.0

2.5

0

TEC — el cm^{-2} × 10^{16}

0.6

0.6

1053-1105 UT
24 FEBRUARY 1977

1

1

10

2

4

4

2

2

2

0.6

1

300

250

200

150

100

50

0

ALTITUDE — km

-300   -200   -100   0   100   200   300

DISTANCE FROM CHATANIKA — km

FIGURE 1. WIDEBAND II AND CHATANIKA DATA,
2/24/77

LMSC/D626959

I/O=1
I/O=2
I/O=4
I/O=16
ITCH
MEA
MEB
MEC
MED

STST	1142:40	1143:40	1144:40	1145:40	1146:40	1147:40	1148:40
LCN	219.42	209.45	203.05	198.71	195.49	193.00	191.44
LAT	78.13	75.00	71.64	69.26	67.92	161.67	158.83
ALT	860.13	969.78	1085.50	1205.62	1332.75	1453.03	1596.83
ILA	78.96	75.07	71.38	67.91	64.66	661.65	58.86
MLT	22.69	22.91	23.05	23.15	23.21	23.27	23.31

CHATANIKA

FIGURE 2. S3-3 SATELLITE DATA, 2/24/77

FIGURE 3.

FIGURE 4.

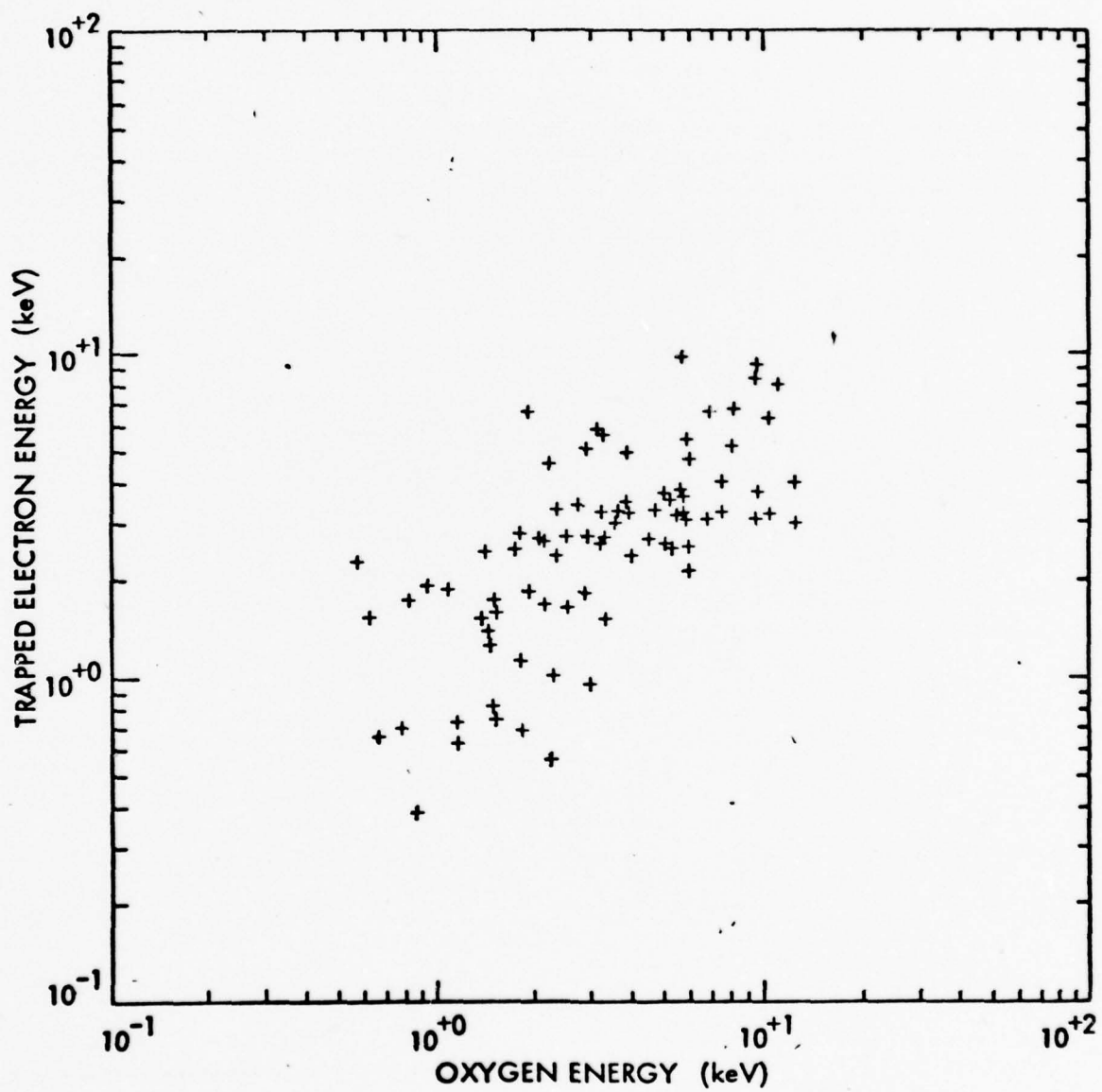11

FIGURE 5.

FIGURE 6.

13

FIGURE 7.

14
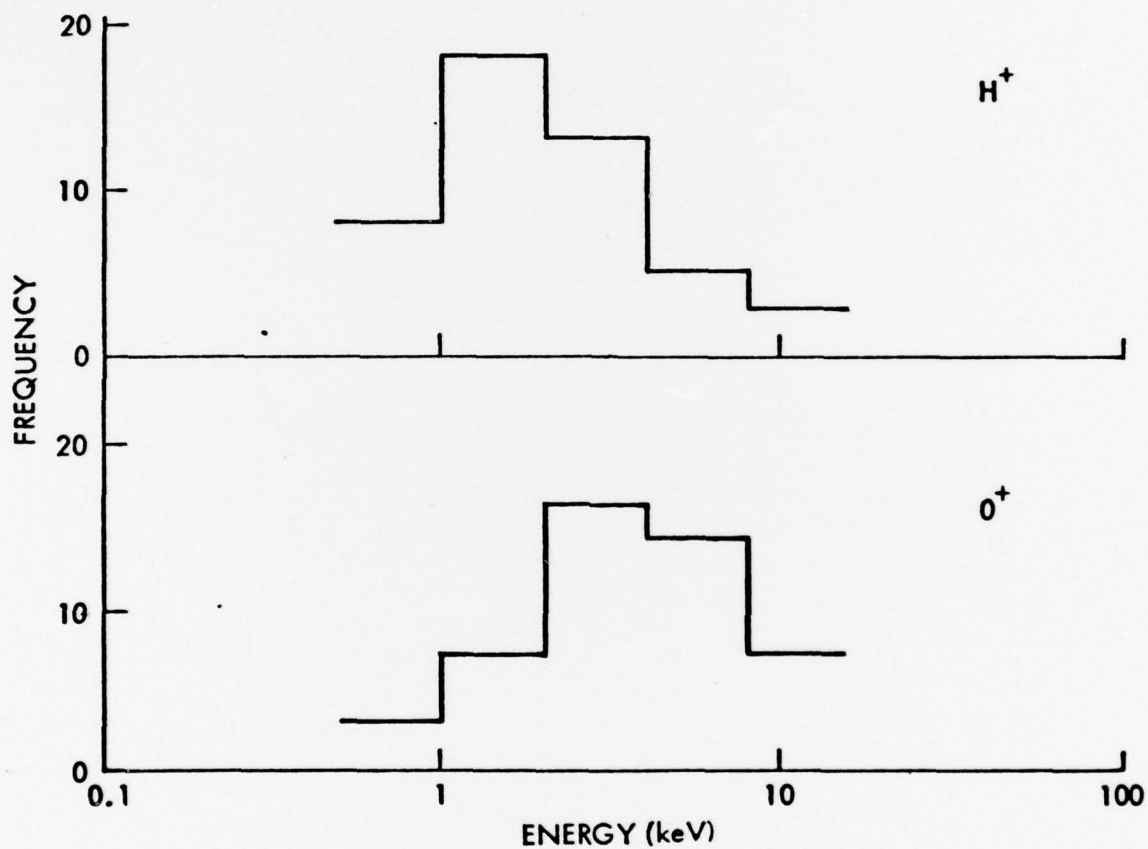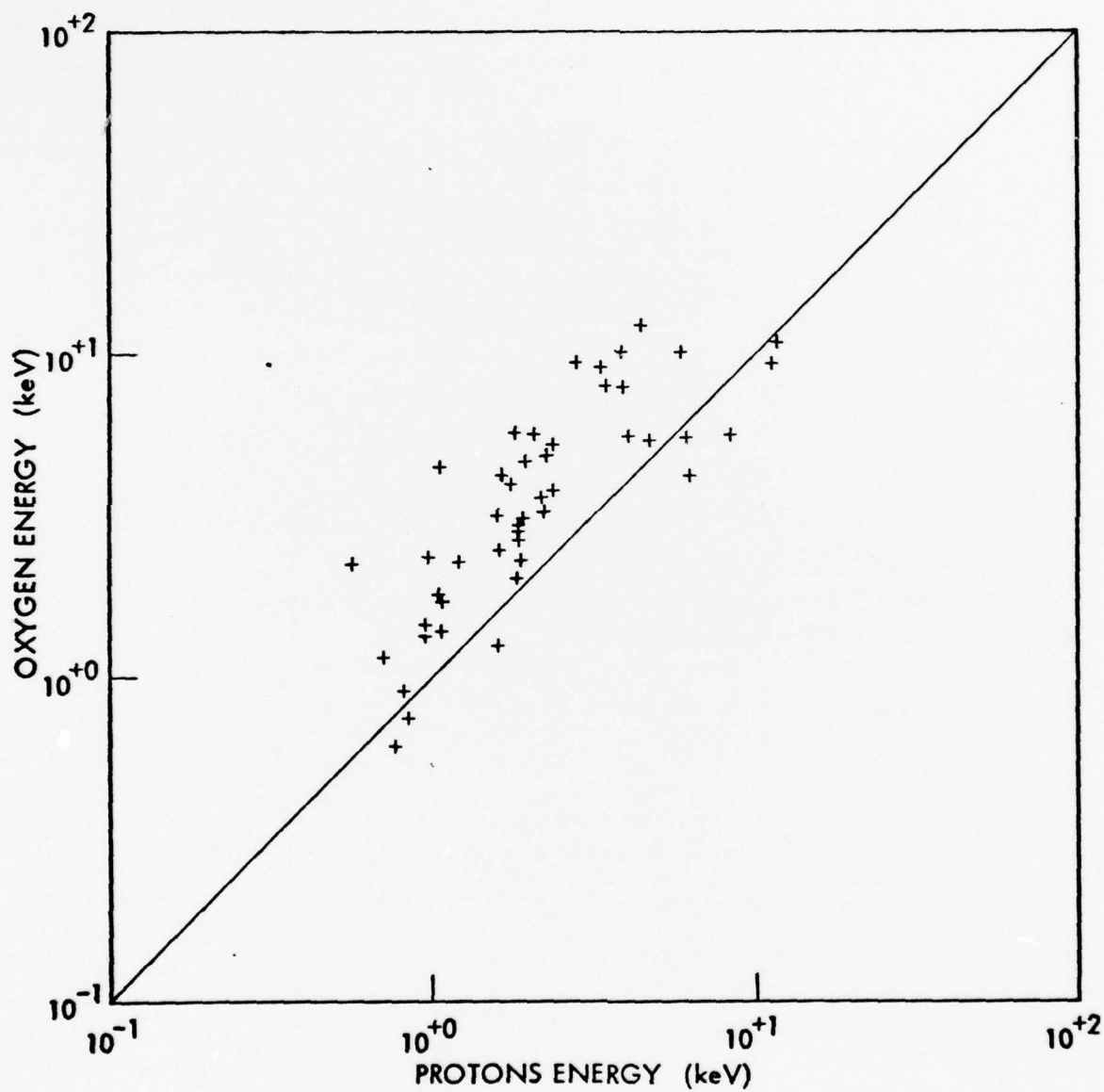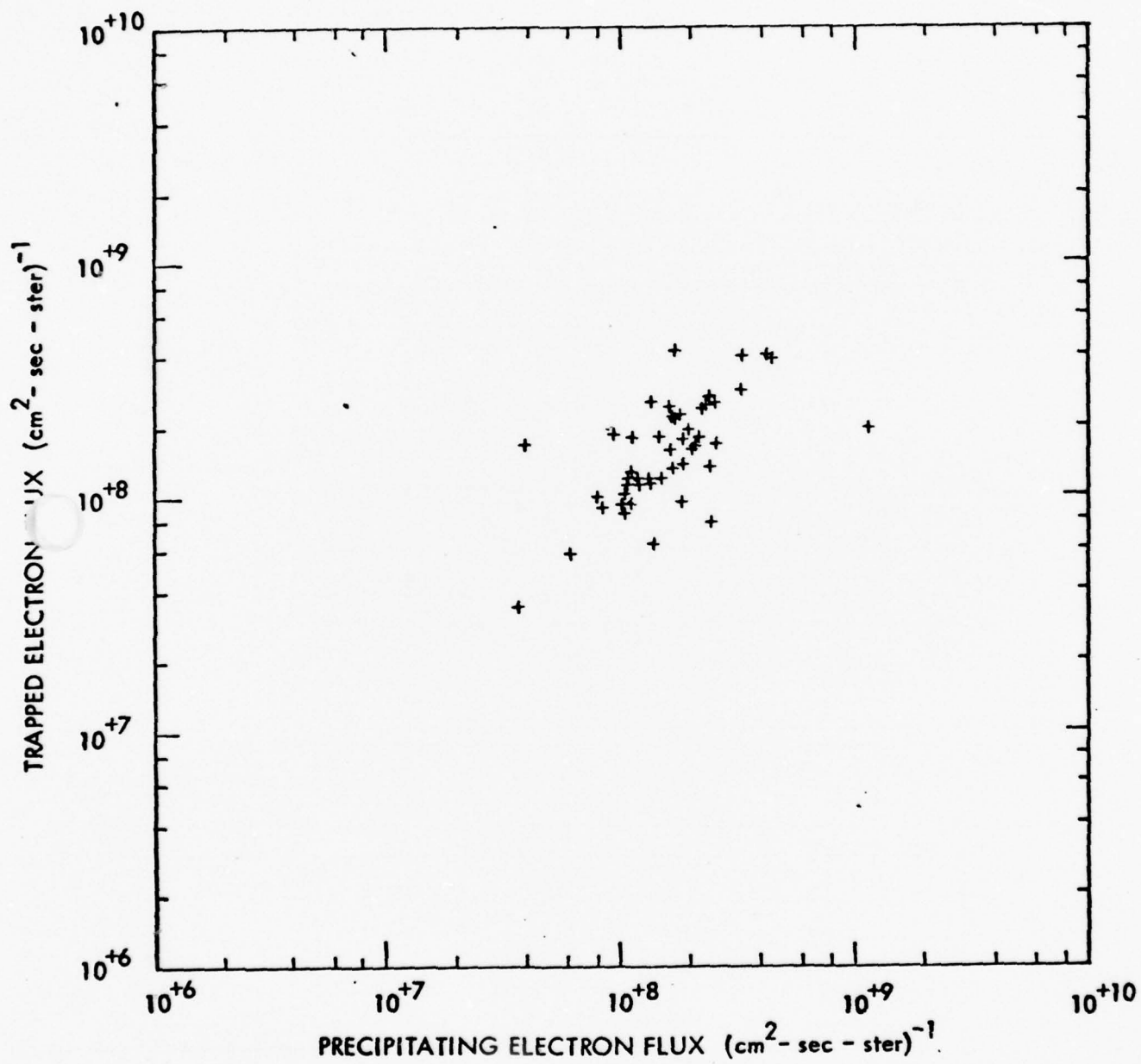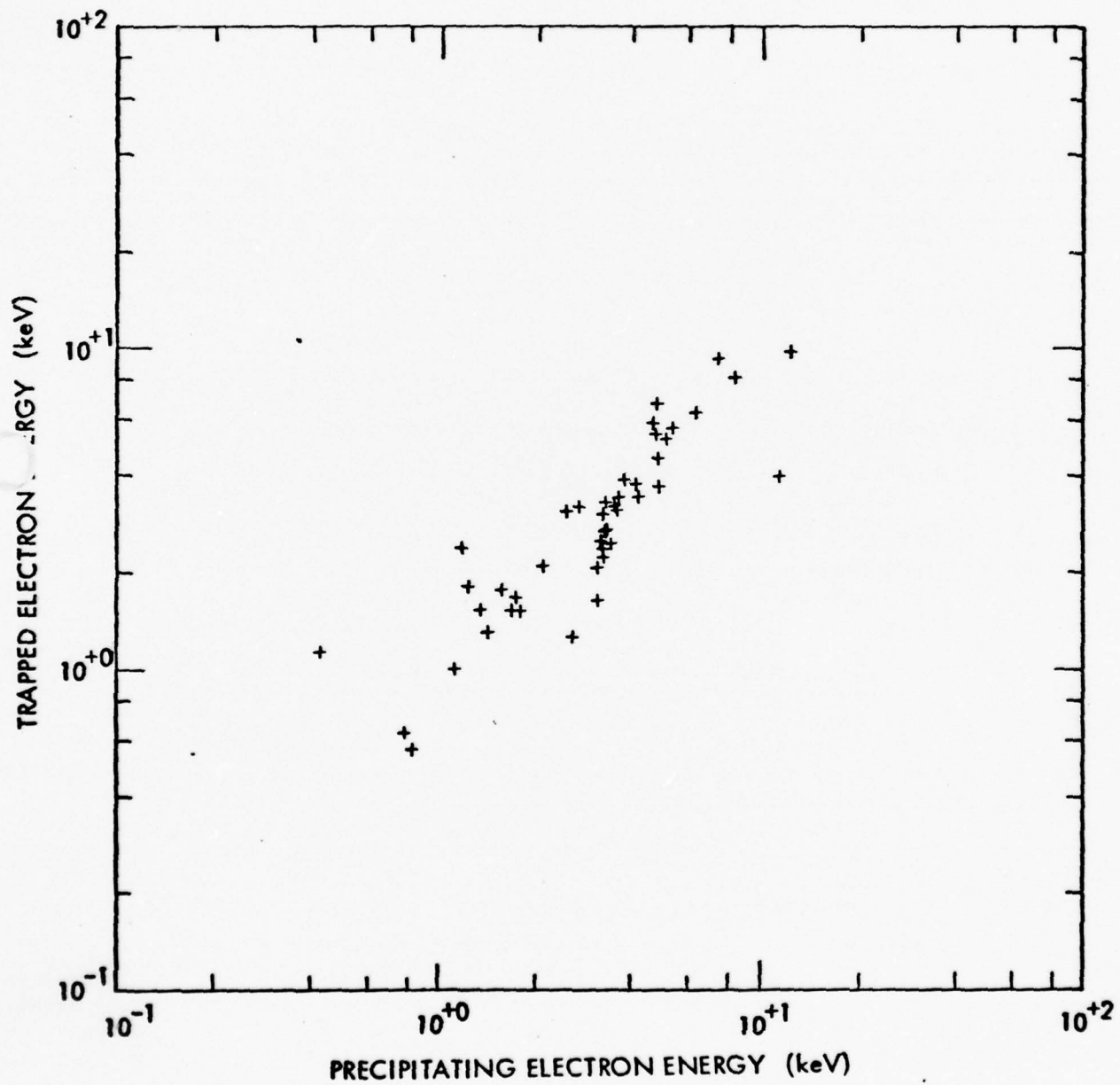
AN IONOSPHERIC PRECURSOR OF AN AURORAL SUBSTORM
AS OBSERVED BY THE CHATANIKA RADAR AND THE S3-3 SATELLITE

by

R. R. Vondrak
Radio Physics Laboratory
SRI International
Menlo Park, CA 94025

R. D. Sharp
R. G. Johnson
Lockheed Palo Alto Research Laboratory
Palo Alto, CA 94304

F. S. Mozer
C. A. Catell
R. B. Torbert
Space Sciences Lab
University of California
Berkeley, CA 94720

J. F. Fennell
P. F. Mizera
The Aerospace Corporation
Ivan A. Getting Laboratories
Los Angeles, CA 90009

Introduction

Measurements of the ionospheric plasma by the incoherent-scatter radar at Chatanika, Alaska have identified a transient phenomenon that may be a precursor of some auroral substorms. At times a narrow pillar (or wall) of ionization forms in the quiet auroral ionosphere. This feature, a flux tube of enhanced ionization extending from the E-region into the F-region, may persist for tens of minutes and move slowly in latitude. The altitude profile of ionization in such a structure is unlike that found in the diffuse or discrete aurora. The pillar coincides with a latitudinal reversal in the east-west electric field, and the pillar formation may result from the accumulation of ionization at the reversal. With time the profile steepens with increased ionization at lower altitudes, and an auroral substorm may develop.

Such a sequence of events was observed on the night of 1 March 1977. Fortunately, the S3-3 satellite passed near Chatanika during the growth of the ionization pillar, approximately 15 minutes prior to the substorm onset. The region of the ionization pillar (< 1° of latitude) was found to be the only high-latitude location in which keV electron precipitation was observed by the S3-3 charged particle detectors. The satellite measurements of charged-particle fluxes and electric fields can be combined with the radar measurements to obtain a detailed description of this auroral feature.

Chatanika Radar Measurements

During the night of 1 March 1977 the Chatanika radar was operated in an elevation-scan mode to map the two-dimensional (altitude, latitude) spatial variation of ionization and other electrical parameters in the auroral ionosphere. A region of approximately 600 km horizontal extent was surveyed with a spatial resolution of about 10 km and a temporal resolution of approximately 12 minutes.

The ionization pillar observed on 1 March 1977 is shown in Figures 1 to 6. These measurements were made during a one-hour period around local midnight (1000 UT). Prior to these measurements little ionization, visual aurora, or magnetic activity were evident at Chatanika.

In Figure 1 is shown the initial appearance of the ionization pillar about 250 km north of Chatanika. The measured ionization differs from that seen in either the diffuse aurora or discrete arcs because of the high altitude of the E-region maximum ($10^5/cm^3$ at 140 km) and the extent of substantial electron density into the F-region ($8 \times 10^4/cm^3$ at 240 km).

In the next scan (Figure 2) the pillar has moved southwards. A remarkable feature of the ionization pillar is that it appears to coincide with a latitudinal reversal of the east-west electric field. The horizontal component of the line-of-sight velocity measured during this scan is shown in Figure 3. On both sides of the pillar the direction of ionospheric drift is such as to drive the ambient ionization into the pillar.

The following scans (Figures 4-6) show the development of the pillar into a dynamic active aurora. During the pillar development magnetic conditions were very quiet. A large negative bay appeared at the time the pillar changed into a dynamic aurora. The all-sky camera photographs showed no visual aurora during the time the pillar was present. Dynamic auroral arcs appeared suddenly at 1030 UT.

S3-3 Satellite Measurements

The S3-3 groundtrack over Alaska during orbit 1900 on 1 March 1977 is shown in Figure 7. The satellite crossed the latitude of Chatanika at approximately 1013 UT at an altitude of about 1600 km. In Figure 7 the latitudinal extent of Chatanika E-region measurements at an altitude of 100 km are indicated by the solid line.

A summary of some of the S3-3 satellite data is shown in Figure 8. The bottom panel shows the electron energy-time spectrogram from the Aerospace detector. The spectrogram shows that significant fluxes of auroral keV electrons were detected in only a very narrow latitudinal region. This region was at the same geomagnetic latitude as the ionization pillar that was located approximately 150 km west of the satellite groundtrack. Although low-energy electrons (< 500 eV) were detected north of this feature, the ionization pillar was the only region in which keV electron precipitation was observed.

Measurements of AC electric fields by the Berkeley S3-3 instrumentation are shown in the upper panel of Figure 8. There was a marked reduction in AC noise over the electron precipitation region; north of it there was a broad region of VLF hiss. Preliminary data from the Berkeley DC electric field probes indicate that the meridional electric field was southward and small ($\sim$ 20 mV/m) in this region.

The final measurement shown in Figure 8 is the flux of 235 keV electrons (center plot). It can be seen that the trapping boundary of energetic electrons is at the equatorward edge of the ionization pillar.

A more detailed representation of the auroral electron fluxes is shown in Figure 9. These data are from two channels of the Lockheed electron detectors that have an energy bandwidth of approximately 50% of the indicated center energy. Because the satellite spin period is about 20 sec, a complete pitch-angle survey corresponds to about 50 km of groundtrack distance. The upper plot of Figure 9 indicates the pitch angle of the detected electrons; a downward arrow indicates precipitating electrons. The satellite data have been plotted versus geomagnetic latitude on a scale corresponding to those used for the Chatanika data in Figures 1 to 6. For reference, the locations of the pillar and equatorward appendage (toe) during the scan closest to the S3-3 pass (Figure 4) are also shown. It can be seen that there is an excellent agreement between the location of the ionization pillar observed with the Chatanika radar and the region of 3.3 keV auroral electron fluxes. In the toe equatorward of the pillar no significant electron fluxes were detected. The only exception was a

narrow beam of upward-moving 150 eV electrons detected equatorward of the pillar.

The Aerospace measurements of ion fluxes are shown in Figure 10. The pitch angle of the detected ions is indicated in a manner analogous to Figure 9. In the pillar the Aerospace detectors were monitoring upward moving ions; no significant fluxes were detected. Equatorward of the pillar there were significant fluxes of 3.9 keV ions and a spectral hardening of the precipitating ion energy distribution. Because no precipitating electrons were found in this region by the Lockheed detectors, these keV ions were the primary energy input into the ionosphere in the toe equatorward of the pillar.

Discussion

The ionization pillar detected by the Chatanika radar is unusual because of its narrow latitudinal extent and its possible role as a precursor of an auroral substorm. It differs from the discrete arc that brightens at the onset of a conventional auroral substorm in several respects. The pillar is a subvisual feature not detectable on all-sky camera photographs. Also, its formation is followed by dynamic auroral activity (arcs and surges) that may not be as intense as that accompanying a normal auroral substorm.

The preliminary analysis of the combined Chatanika radar and S3-3 satellite data from 1 March 1977 have identified the following characteristics:

1. The pillar is narrow in latitude (< 1° or 100 km), but extends in geomagnetic longitude over at least 150 km. Therefore, it is really a wall of ionization rather than a pillar. It is located at the equatorward edge of the auroral region and at the trapping boundary. It is the only high-latitude location of keV electron precipitation.

2. The pillar coincides with a latitudinal reversal in the east-west electric field. This ionospheric electric field configuration causes ambient ionization to drift towards the pillar flux tube, although the relative importance of transport compared to local production by particle precipitation has not yet been evaluated.

3. Equatorward of the pillar significant fluxes of precipitating keV ions are present. No precipitating electrons are present there, although there may be significant fluxes of upward-streaming, cold (100 eV), electrons.

Some interesting questions regarding this feature have not yet been answered. Why does keV electron precipitation occur over such a narrow region and only at the equatorward edge of the auroral oval? What is the relation of the pillar electrical configuration to auroral acceleration processes? What role does the ionization pillar have in the development of an auroral substorm?

It is expected that a more complete understanding of the relation of this feature to auroral morphology and dynamics can be obtained by a complete analysis of the combined radar and satellite data sets.
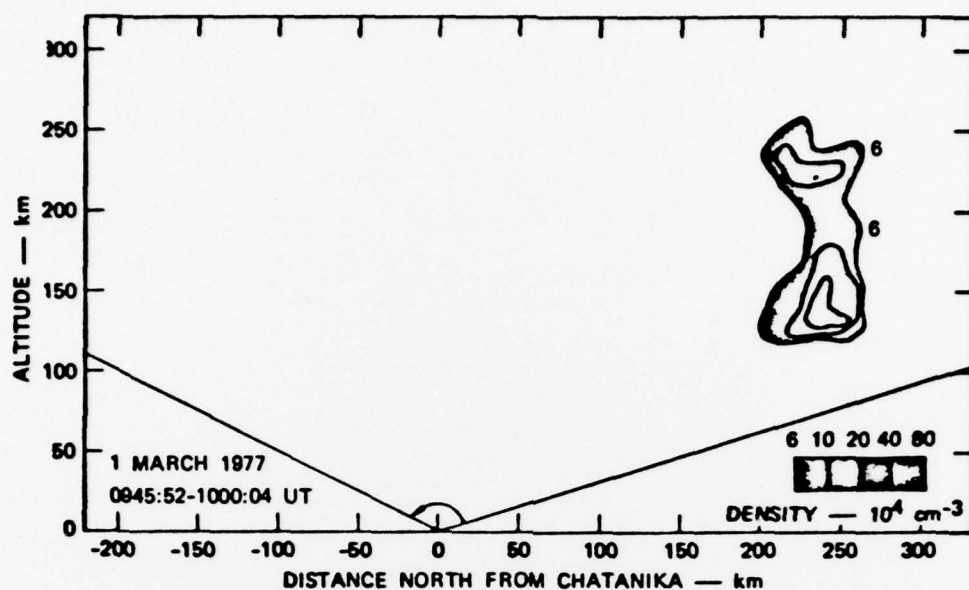
Figure 1. Contour Map of electron number density made
from 0945:52 to 1000:04 UT on 1 March, 1977.
The radar scanned southward between the
indicated limits.
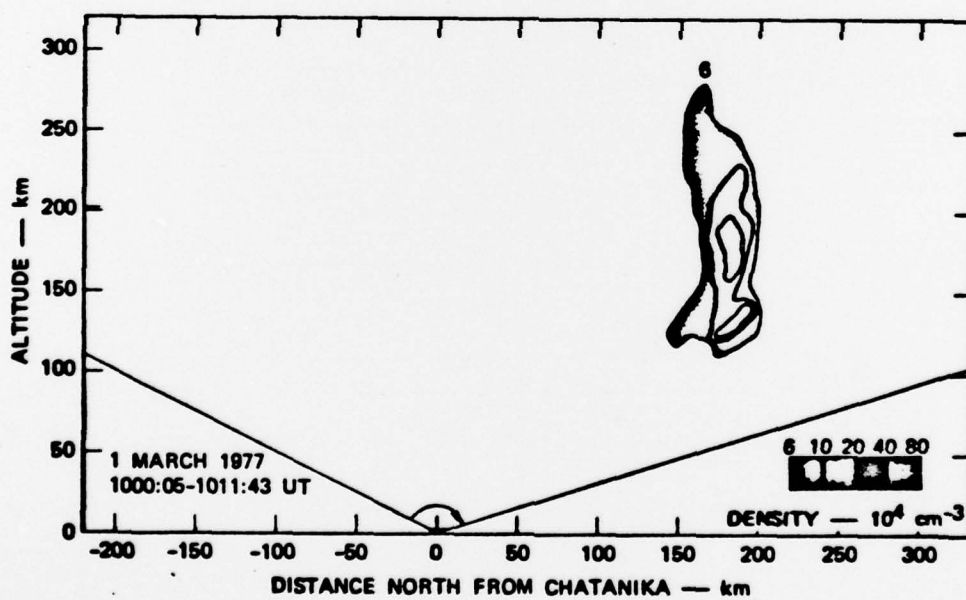
Figure 2. Electron density measured during scan following
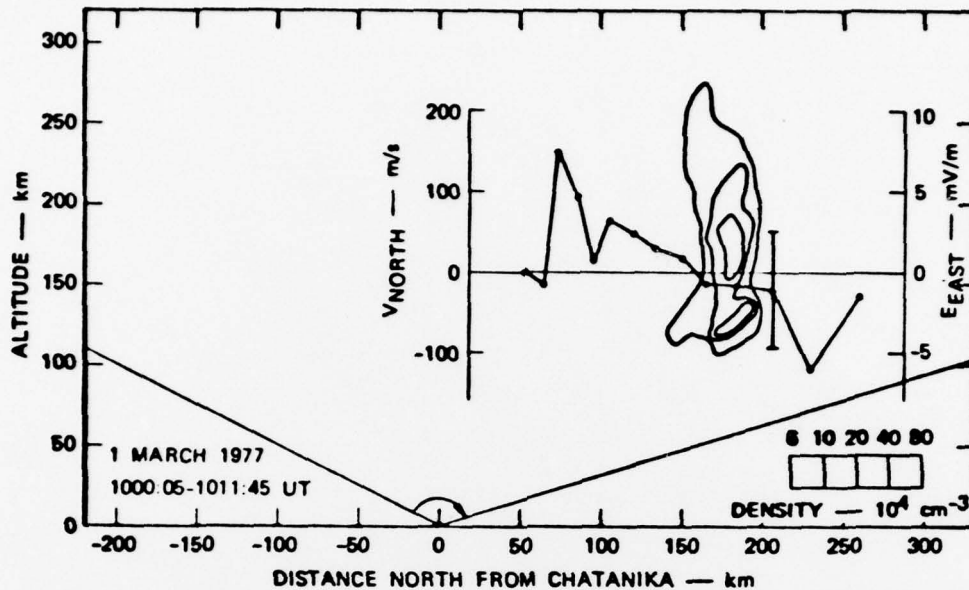that shown in Figure 1.

Figure 3. Latitudinal variation of northward drift
(eastward electric field) at an altitude
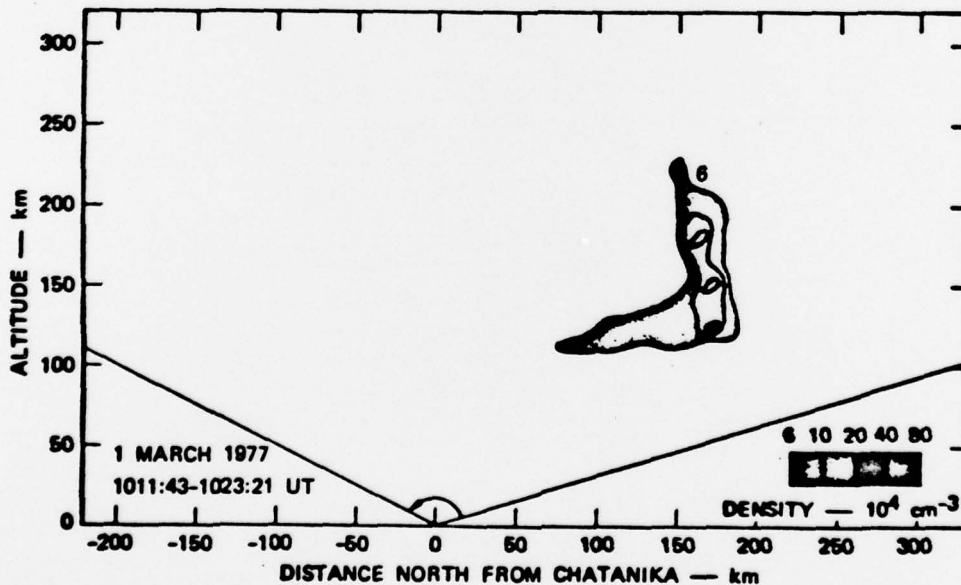of 170 km during scan shown in Figure 2.

Figure 4. Electron density measured during scan following
that shown in Figure 2. Increased ionization
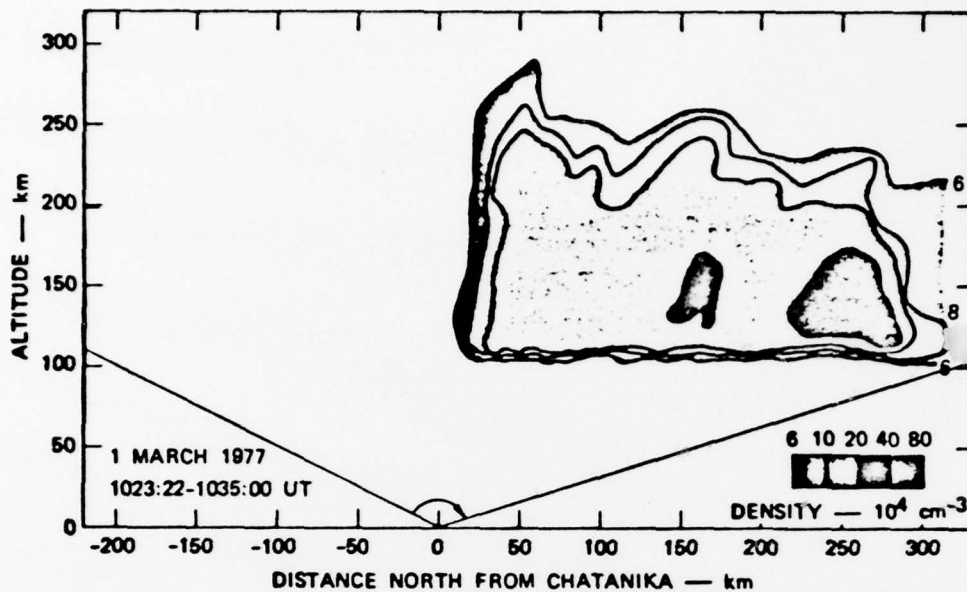is evident in the E-region equatorward of the
pillar.

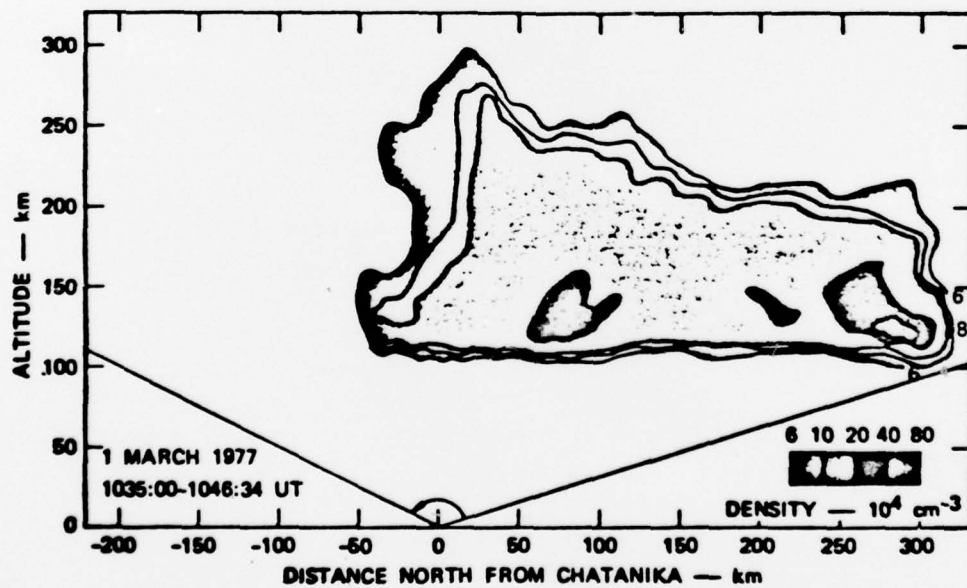Figure 5. Electron density measured during scan following that shown in Figure 4.

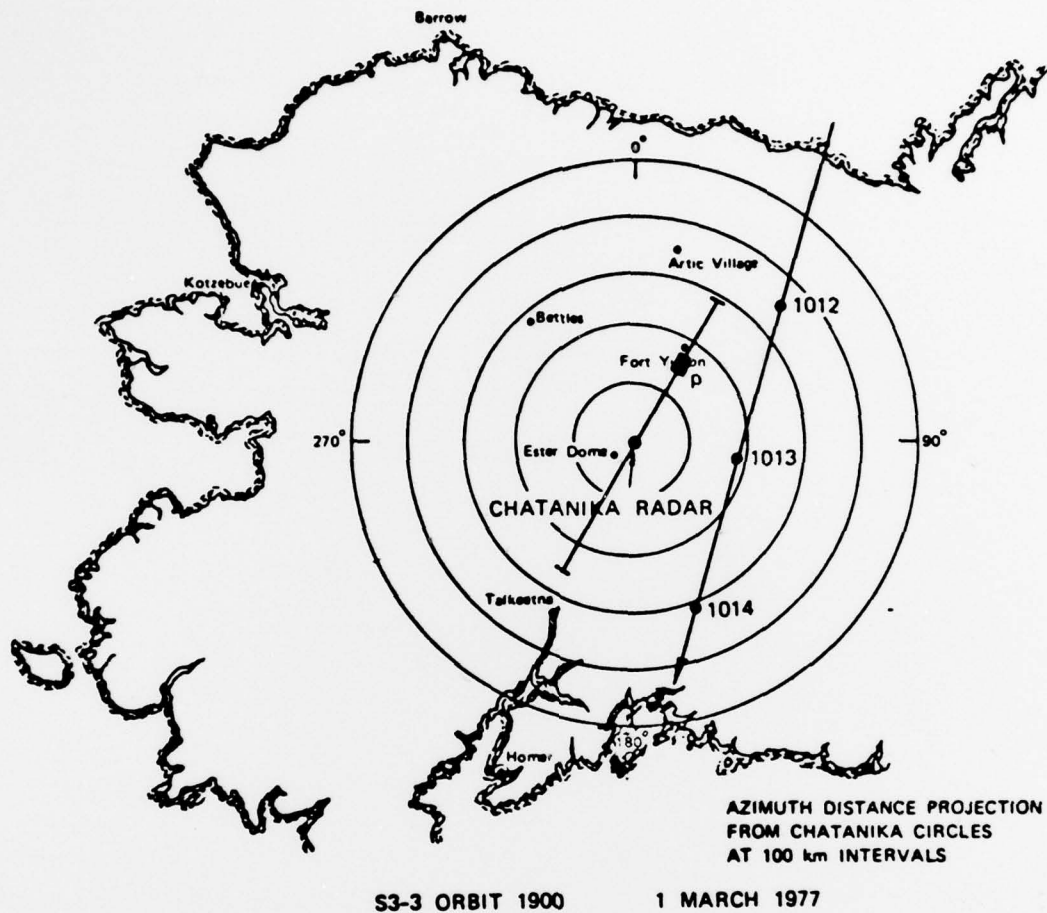Figure 6. Electron density measured during scan following that shown in Figure 5.

AZIMUTH DISTANCE PROJECTION
FROM CHATANIKA CIRCLES
AT 100 km INTERVALS

S3-3 ORBIT 1900   1 MARCH 1977

Figure 7.   S3-3 groundtrack on 1 March 1977. Also
indicated is the location of the ionization
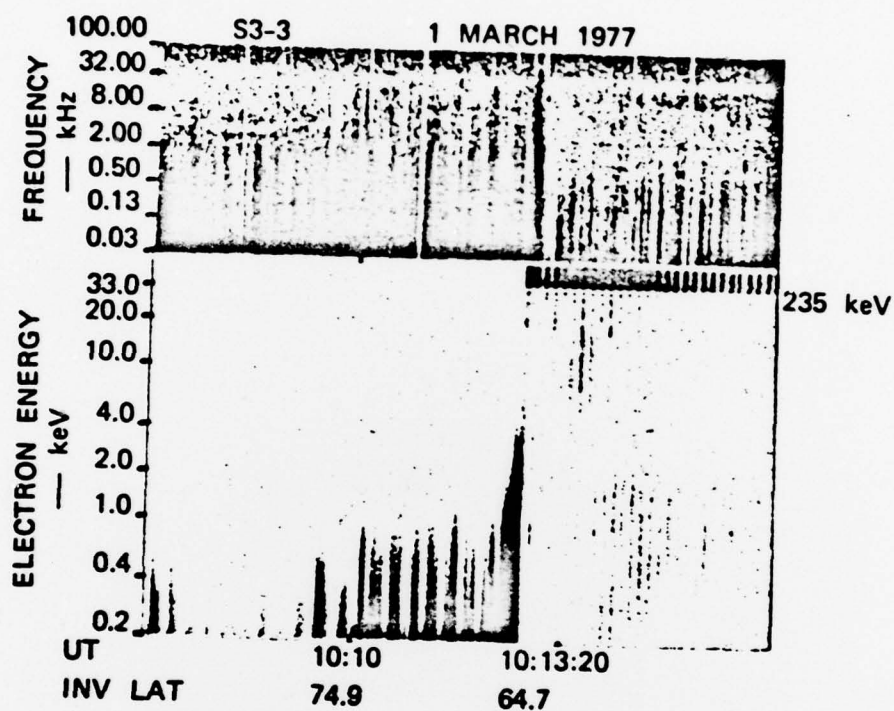pillar (p) at approximately 1014 UT.

A-9

Figure 8. Summary of S3-3 measurements of AC electric fields, energetic (235 keV) trapped electrons, and auroral electrons (0.17-33keV).
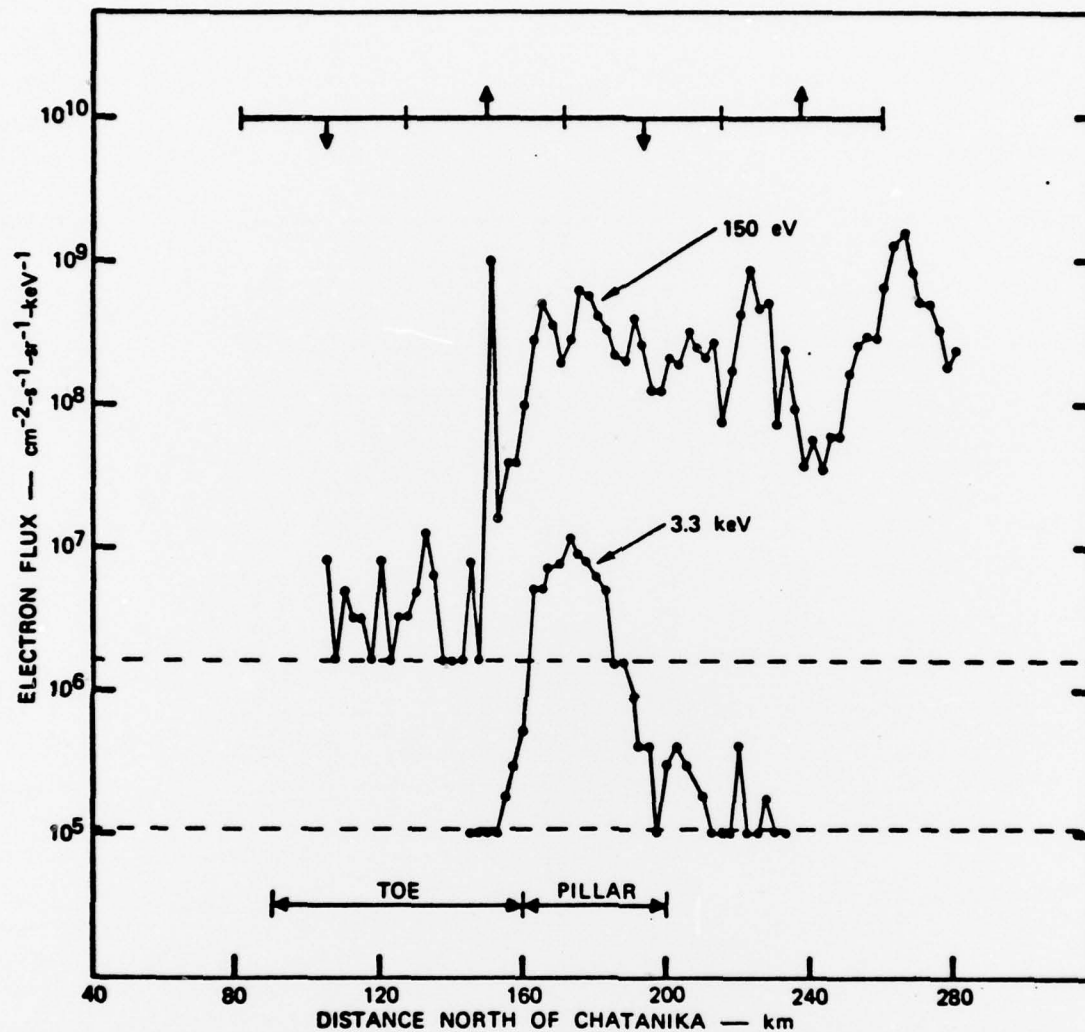
Figure 9. Auroral electron fluxes measured by the
Lockheed detectors simultaneous with the
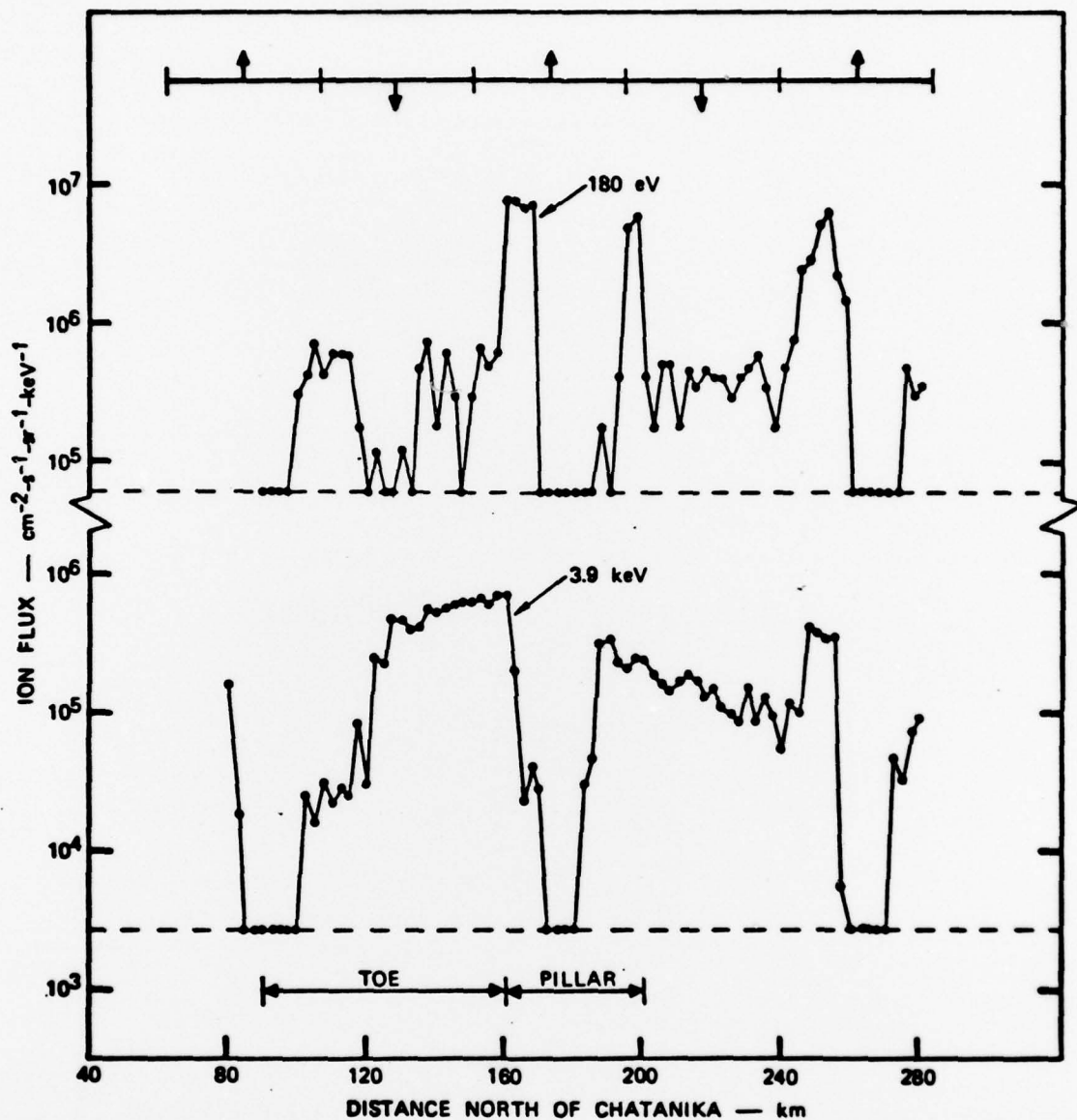Chatanika measurements shown in Figure 4.

Figure 10. Ion fluxes measured by the Aerospace
detectors simultaneous with the Chatanika
measurements shown in Figure 4.

Department of Defense

Director
Defense Communications Agency
8th Street and South Courthouse Road
Arlington, Virginia 22204

   1 cy   ATTN: MEECN Office

Defense Documentation Center
Cameron Station
Alexandria, Virginia 22314

   12 cys ATTN: TC

Director
Defense Nuclear Agency
Washington, D.C. 20305

   2 cys   ATTN: RAAE

Department of Commerce

U.S. Department of Commerce
Office of Telecommunications
Institute for Telecommunication Sciences
National Telecommunications and Information
 Administration
Boulder, Colorado 80303

   1 cy   ATTN: W.F. Utlaut

Department of the Army

Commander/Director
Atmospheric Sciences Laboratory
U.S. Army Electronics Command
White Sands Missile Range, New Mexico 88002

   1 cy   ATTN: DRSEL-BL-SY-S
                  F.E. Niles

Department of the Navy

Chief of Naval Operations
Department of the Navy
Washington, D.C. 20350

   1 cy   ATTN: NOP 985

Chief of Naval Research
Department of the Navy
800 North Quincy Street
Arlington, Virginia 22217

 1 cy ATTN: Code 465, R.G. Joiner
 1 cy ATTN: Code 427, H. Mullaney

Commander
Naval Electronic Systems Command
Department of the Navy
Washington, D.C. 20360

 1 cy ATTN: PME-117T
 1 cy ATTN: PME 117-21

Director
Naval Ocean Systems Center
Electromagnetic Propagation Division
271 Catalina Boulevard
San Diego, California 92152

 1 cy ATTN: Code 2200, W.F. Moler
 1 cy ATTN: Code 2200, John Bickel

Director
Naval Research Laboratory
4555 Overlook Avenue, S.W.
Washington, D.C. 20375

 1 cy ATTN: Code 7700, Timothy P. Coffey
 2 cys ATTN: Code 7750, John Davis

Commander
Naval Surface Weapons Center (White Oak)
Silver Spring, Maryland 20910

 1 cy ATTN: Technical Library

Office of Naval Research Branch Office (Pasadena)
1030 East Green Street
Pasadena, California 91106

 1 cy

Department of the Air Force

Commander
Air Force Geophysical Laboratory, AFSC
L.G. Hanscom Air Force Base, Massachusetts 01731

 1 cy ATTN: OPR, James Ulwick
 1 cy ATTN: LKB, W. Swider

Director
Air Force Technical Applications Center
Patrick Air Force Base, Florida 32920

   1 cy   ATTN: TD
   1 cy   ATTN: HQ 1035th TCHOG/TFS

Department of Defense Contractors

General Electric Company
TEMPO - Center for Advanced Studies
816 State Street
Santa Barbara, California 93102

   1 cy   ATTN: Warren S. Knapp
   1 cy   ATTN: DASIAC

Pacific-Sierra Research Corporation
1456 Cloverfield Boulevard
Santa Monica, California 90404

   1 cy   ATTN: E.C. Field

Pennsylvania State University
Ionospheric Research Laboratory
College of Engineering
318 Electrical Engineering - East Wing
University Park, Pennsylvania 16802

   1 cy   ATTN: John S. Nisbet

R&D Associates
4640 Admiralty Way
Marina Del Rey, California 90291

   1 cy   ATTN: R. Lelevier
   1 cy   ATTN: R. Turco

The Rand Corporation
1700 Main Street
Santa Monica, California 90406

   1 cy   ATTN: Cullen Crain

Stanford Research Institute
333 Ravenswood Avenue
Menlo Park, California 94025

   1 cy   ATTN: Ray L. Leadabrand